Characterization of the laser crystal $Nd:GdVO_4$

Huaijin Zhang, Junhai Liu, Jiyang Wang, Changqing Wang, Li Zhu, Zongshu Shao, Xianlin Meng, Xiaobo Hu, and Minhua Jiang

National Laboratory of Crystal Materials and Institute of Crystal Materials, Shandong University, Jinan, 250100, China

Yuk Tak Chow

Department of Electronic Engineering, City University of Hong Kong, Tat Chee Avenue, Kowloon, Hong Kong, China

Received February 26, 2001; revised manuscript received July 17, 2001

$Nd:GdVO_4$ crystal was grown by the Czochralski method. The absorption and fluorescence spectra of the crystal were measured at room temperature. The thermal expansion and the specific heat of the crystal were also measured. Laser outputs at 1.06 and 1.34 μm were achieved when a $Nd:GdVO_4$ crystal sample with a high Nd doping concentration was pumped by a low-power laser diode (LD) at 808.5 nm, and visible green and red laser outputs of intracavity frequency doubling at 0.53 and 0.67 μm were also achieved when nonlinear $KTiOPO_4$ and LiB_3O_5 crystal, respectively, were used. The highly Nd-doped $Nd:GdVO_4$ crystal was pumped by a high-power LD, and a greater than 5-W laser output power at 1.06 μm was obtained. A low-Nd-doping concentration $Nd:GdVO_4$ crystal sample was pumped by a high-power LD, yielding laser output powers at 1.06 and 0.53 μm; 0.53-μm green laser output was obtained when a $KTiOPO_4$ crystal was used, and the output beam's values were $M^2 = 1.76$ at an output power of 14.3 W at 1.06 μm and $M^2 = 1.55$ at an output power of 3.3 W at 0.53 μm. Acousto-optical Q-switched laser outputs at 1.06 and 0.53 μm were also achieved. A thermal lens made from a $Nd:GdVO_4$ crystal was measured; it was weaker than that of a $Nd:YVO_4$ crystal. Some important material parameters, such as temperature-induced changes in refractive index, material constant, thermal-stress resistance figure of merit, and power per unit length at the stress fracture limit, have been estimated.

OCIS codes: 140.0140; 160.0160.

1. INTRODUCTION

In recent years laser diode–(LD)-pumped solid-state lasers have attracted great attention owing to the excellent properties, such as high efficiency, simplicity, compactness, and good frequency stability, of the lasers. There are many important military and industrial applications of these lasers as well as applications for medical treatment, optical communications, and scientific research. The laser crystal is one of the most important components of a LD-pumped solid-state laser; it can determine the efficiency of the laser. The zircon structure neodymium-doped vanadate crystal $Nd:YVO_4$,[1–6] has proved to be an excellent laser crystal because of its good lasing properties, and high conductivity, and it is now widely used. $Nd:GdVO_4$ crystal was introduced as a laser material by Zaguniennyi *et al.*[7] Its space group is $14_1/amd$, the same as that of YVO_4. Some experiments have shown that $Nd:GdVO_4$ crystal is also an efficient LD-pumped solid-state laser crystal.[7–10] The thermal conductivity of $Nd:GdVO_4$ along the $\langle 110 \rangle$ direction is comparable with that of Nd:YAG,[11] and it is almost two times greater than that of $Nd:YVO_4$.[12] Therefore, $Nd:GdVO_4$ is also more competitive in high-power laser generation. But the high-power LD pumping of $Nd:GdVO_4$ lasers at 1.06 μm and operation of intracavity frequency-doubled green and especially red lasers have been largely ignored. In this paper we characterized the $Nd:GdVO_4$ crystal grown by the Czochralski method. The absorption and fluorescence spectra of $Nd:GdVO_4$ crystal were measured at room temperature, and the laser output of a highly Nd-doped $Nd:GdVO_4$ crystal at 1.06 and 1.34 μm and the double frequency output at 0.53 and 0.67 μm with nonlinear $KTiOPO_4$ (KTP) and LiB_3O_5 (LBO) crystals were achieved. Laser output of a low-Nd-doping concentration $Nd:GdVO_4$ crystal at 1.06 and 0.53 μm and acousto-optical Q switching at 1.06 and 0.53 μm were also achieved with a high-power LD. The thermal lens of a $Nd:GdVO_4$ crystal was measured.

2. CRYSTAL AND EFFECTIVE SEGREGATION COEFFICIENT

We used the chemical compounds V_2O_5, Gd_2O_3, and Nd_2O_3 with 99.99% purity to grow series $Nd:GdVO_4$ crystals. These compounds were weighted according to the following ratios: $Nd_{0.02}Gd_{0.98}VO_4$ and $Nd_{0.0064}Gd_{0.9936}VO_4$. The polycrystalline materials were synthesized by the solid-state reaction method.

A $Nd:GdVO_4$ single crystal was grown in an iridium crucible by the Czochralski method. The growth conditions of the $Nd:GdVO_4$ crystal were similar to those of the $Nd:YVO_4$ crystal.[13]

The x-ray powder diffraction method was used to measure the structure and lattice constants of $Nd:GdVO_4$ crystal at room temperature. An as-grown $Nd:GdVO_4$ crystal (Nd doping concentration, 2 at. % in the melt) was ground into powder and used as a sample.

0740-3224/2002/010018-10$15.00

Table 1. Effective Segregation Coefficients (K_{eff}) of Nd, Gd, and V Ions in Nd:$GdVO_4$ Crystal

Element	K_{eff}
Nd	0.781
Gd	1.021
V	0.997

The results of x-ray analysis showed that Nd:$GdVO_4$ crystal has a structure like that of $ZrSiO_4$ in the space group $I4_1/amd$. The lattice constants of the as-grown Nd:$GdVO_4$ crystal are $a = b = 0.7212(1)$ nm and $c = 0.6350(1)$ nm. The lattice constants of Nd:$GdVO_4$ crystal are in agreement with the Joint Committee for Power Diffraction Standards data for $GdVO_4$ ($a = b = 0.72126$ nm, $c = 0.63483$ nm).[14]

We used x-ray fluorescence analysis to measure the concentrations of Nd, Gd, and V in $GdVO_4$ crystal grown from a 2-at. % Nd-doped Nd:$GdVO_4$ polycrystal, and based on the results of the analysis, we could calculate the effective segregation coefficients of the elements involved in in Nd:$GdVO_4$ crystal growth. The measured sample was cut from the upper part of an as-grown Nd:$GdVO_4$ crystal boule that had been grown for the first time from the new 2-at. % Nd-doped Nd:$GdVO_4$ polycrystalline material, and we used the 2-at. % Nd-doped Nd:$GdVO_4$ polycrystalline material as a standard for comparison.

Table 1 lists the effective segregation coefficients of Nd, Gd, and V ions in the growth of 2-at. % Nd-doped $GdVO_4$ crystals. The effective segregation coefficient of Nd in a Nd:$GdVO_4$(0.78) crystal is larger than that of a Nd:YVO_4(0.63) crystal.[15] The effective segregation coefficients of V and Gd ions are near 1.

3. THERMAL EXPANSION AND SPECIFIC HEAT

Thermal problems are important in the growth of laser crystals. Optical pumping of all-solid-state lasers generates some amount of localized heating of the laser material. Heating has several causes: quantum defects, quenching mechanisms, thermalized terminal laser level(s), and absorption of the pump photons by the host material. Under operating conditions the thermally loaded laser host medium exhibits optical distortions, which include thermal focusing, stress-induced biaxial focusing, and stress-induced birefringence. These thermally induced effects severely degrade the optical quality of a laser beam and eventually limit laser output power. The combined effects of volumetric heating and surface cooling can result in thermal–mechanical failure from stress.

Stress fracture occurs when the stress induced by temperature gradients in a laser material exceeds the tensile strength of the material. The power per unit length at the stress fracture limit is[16]

$$\frac{P_a}{l} = 12R_s\frac{w}{t}, \tag{1}$$

where w/t is the aspect ratio of width to thickness and R_s is a thermal stress resistance figure of merit (FOM) for the material ($R_s = \sigma_{max}M_s$, where σ_{max} is the maximum surface stress at which fracture occurs and M_s is a material constant). The thermal stress resistance FOM is valid for a given flaw size and depends on the intrinsic properties of the material. In most cases it is useful to use M_s as a material constant for material comparisons. The material constant can be expressed as

$$M_s = (1 - \nu)(k/\alpha E), \tag{2}$$

where ν is the Poisson ratio, k is the thermal conductivity, α is the thermal expansion coefficient, and E is Young's modulus. From Eq. (2), one can see that the material constant depends only on the intrinsic properties of the material. The material constant is an important value that determines resistance to thermal stress. To calculate M_s we need to know all four parameters. For $GdVO_4$, the thermal conductivity has been measured ($k = 11.7\ \mathrm{W\,m^{-1}\,K^{-1}}$). The Poisson ratio and Young modulus are decided by a fourth-order tensor; measuring the two values for $GdVO_4$ is a complex undertaking. (We may use the two values of Nd:YVO_4.) In this paper we report only our measurements of the thermal-expansion coefficients.

The thermal-expansion coefficient is a second-order tensor.[17] For a tetragonal crystal, Nd:$GdVO_4$, there are only two independent principal thermal components, α_1 and α_3. We obtained them by measuring the thermal expansions of the a- and c-oriented crystal samples.

We used differential scanning calorimetry and a thermomechanical analyzer made by Perkin–Elmer to measure the thermal expansion and the specific heat of our samples. The samples of Nd:$GdVO_4$ used for the thermal-expansion experiment were a- and c-oriented crystals with lengths of 2.80 and 2.56 mm, respectively.

Figure 1 shows the thermal-expansion curves of Nd:$GdVO_4$ along the a and the c axes. From this figure we see no anomaly within the measuring temperature range. The thermal-expansion curves are linear within that range, and the average linear thermal-expansion co-

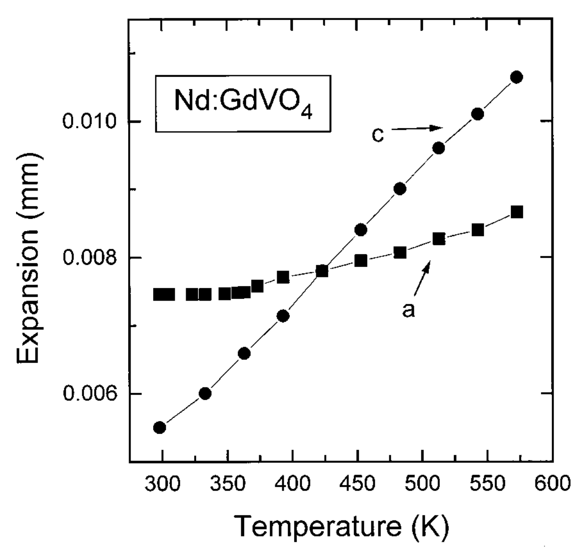

Fig. 1. Thermal expansion of Nd:$GdVO_4$ crystal as a function of temperature. Scan rate, 5 °C/min.

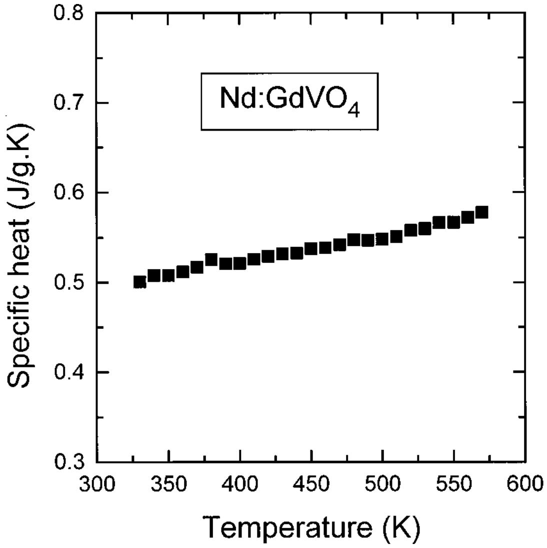

Fig. 2. Dependence of the specific heat of a $Nd:GdVO_4$ crystal on temperature.

efficients of the a and c axes of $Nd:GdVO_4$ measured from 298 to 572.5 K are $\alpha_1 = 1.5 \times 10^{-6}/K$ and $\alpha_3 = 7.3 \times 10^{-6}/K$, respectively.

To estimate the material constant of a $Nd:GdVO_4$ crystal, we used Young's modulus and the Poisson ratio of $Nd:YVO_4$ [Young's modulus is 133 G Pa; the Poisson ratio is 0.33 (Ref. 18)] and repressed those of $Nd:GdVO_4$. We found that material constant M of $Nd:GdVO_4$ crystal is $8.07 \times 10^{-6}\,m^2/s$ and that of $Nd:YVO_4$ is $3.14 \times 10^{-6}\,m^2/s$ [the thermal conductivity of YVO_4 is 5.23 $W\,m^{-1}\,K^{-1}$, and the thermal expansion coefficient is $8.4 \times 10^{-6}/K$ (Ref. 18)].

Specific heat is an important factor that influences the damage threshold of a material in a pulsed laser system.[19] Specific-heat data of solids are generally described by Debye theory in terms of the harmonic frequency spectrum of each atom. It is difficult, however, to calculate the specific heat of a complex $Nd:GdVO_4$ crystal. Figure 2 shows the dependence of the measured specific heat of $Nd:GdVO_4$ on temperature. From this figure we can see that the specific heat is almost linear with temperature in the measured temperature range. The specific heat of $Nd:GdVO_4$ is 32.6 cal/(mol K) at 330 K. It is larger than that of $Nd:YVO_4$ crystal [24.6 cal/(mol K) at 330 K].[20] $Nd:YVO_4$ possesses a high damage threshold, so one could deduce that $Nd:GdVO_4$ crystal should also possess a high damage threshold. Thus, $Nd:GdVO_4$ crystal can be used in a pulsed laser system.

4. ABSORPTION AND FLUORESCENCE SPECTRA

As-grown $Nd:GdVO_4$ crystal boules were cut into crystal samples for spectrum and laser experiments. We used $Nd:GdVO_4$ crystal samples with dimensions of 3 mm $\times$ 3 mm $\times$ 1 mm ($b \times c \times a$; 2-at. % Nd-doping concentration in $Nd:GdVO_4$ melt and 1.56-at. % Nd-doping concentration in $Nd:GdVO_4$) to measure the absorption and fluorescence spectra. The absorption spectrum was measured with a Hitachi-340 recording spectrophotometer, and the light traveled in the direction of the a axis. We used a cw LD at a wavelength of 808.5 nm as the pump source to measure the fluorescence spectrum and an optical spectrum analyzer to record the fluorescence spectra.

The absorption spectrum is shown in Fig. 3 for 1.56-at. % $Nd:GdVO_4$. The measuring wavelength range was 400–850 nm. From Fig. 3 we can see that there are absorption peaks in $Nd:GdVO_4$ (i.e., π polarization and σ polarization) at 808.5 nm. The strength of the π polarization ($E \| c$) absorption is much greater than that of the σ polarization ($E \perp c$) absorption, and the π polarization absorption peak at 808.5 nm is the strongest one among all the absorption peaks in the measuring range. Figure 1 also shows that the full width at half-maximum of $Nd:GdVO_4$ is 4 nm at 808.5 nm. So it is possible to use the LD with the wavelength of 808.5 nm as the pump source for the $Nd:GdVO_4$ crystal.

Figure 4 shows the fluorescence spectrum of $Nd:GdVO_4$ from 850 to 1400 nm. There are three main emission peaks, for wavelengths centered at 912.6 nm ($^4F_{3/2}$

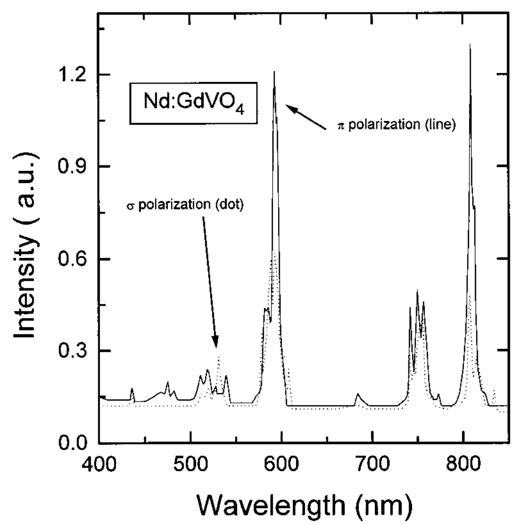

Fig. 3. Absorption spectrum of a $Nd:GdVO_4$ crystal from 400 to 850 nm at room temperature.

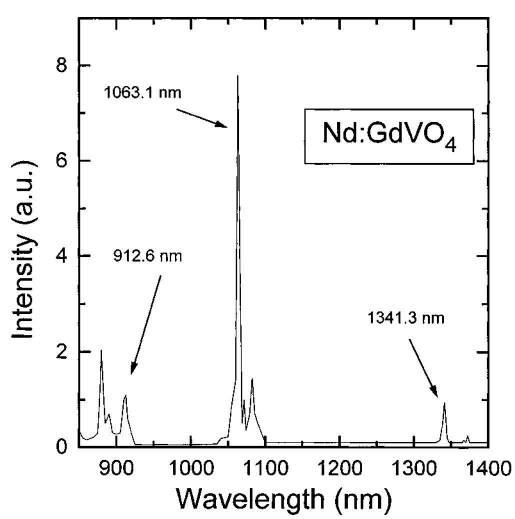

Fig. 4. Fluorescence spectrum of a $Nd:GdVO_4$ crystal from 850 to 1400 nm at room temperature.

$\rightarrow {}^4I_{9/2}$), 1063.1 nm (${}^4F_{3/2} \rightarrow {}^4I_{11/2}$), and 1341.9 nm (${}^4F_{3/2} \rightarrow {}^4I_{13/2}$), and the peak near 1063.1 nm is the strongest of all the peaks. Because the laser output of Nd^{3+} for ${}^4F_{3/2} \rightarrow {}^4I_{9/2}$ is a quasi-three-level system, the maximum Stark split ΔE of ${}^4I_{9/2}$ limits the laser emission of host materials. [There are reabsorption losses in the quasi-three-level system,[21,22] and the resonant loss is proportional to $\exp(-\Delta E/kT)$ (Ref. 23).] The crystal that is usually used in laser emission for ${}^4F_{3/2} \rightarrow {}^4I_{9/2}$ is Nd:YAG, whose maximum Stark split of ${}^4I_{9/2}$ manifold above the ground state is 848 cm^{-1}; but, for Nd:YVO_4, the maximum Stark split is only 433 cm^{-1}. Because of high reabsorption losses and relatively small thermal conductivity, obtaining laser output for ${}^4F_{3/2} \rightarrow {}^4I_{9/2}$ by use of a special Nd:YVO_4 crystal sample at room temperature is a complex operation[24]; the maximum Stark split of Nd:$GdVO_4$ is 409 cm^{-1}.[8] These results show that it is not easy to obtain laser output for ${}^4F_{3/2} \rightarrow {}^4I_{9/2}$ for the small Stark split ΔE of the ${}^4I_{9/2}$ manifold above the ground state of Nd:$GdVO_4$ crystal pumped by a 808.5-nm LD at room temperature. The laser emissions for the ${}^4F_{3/2} \rightarrow {}^4I_{11/2}$ and the ${}^4F_{3/2} \rightarrow {}^4I_{13/2}$ manifolds are four-level systems; one may get laser output for wavelengths of 1063 and 1340 nm more easily. So, in this study, we obtained laser output of 1063 nm (laser emissions for the ${}^4F_{3/2} \rightarrow {}^4I_{11/2}$ manifold) and 1340 nm (laser emissions for the ${}^4F_{3/2} \rightarrow {}^4I_{13/2}$ manifold), not of 912.4 nm (laser emissions for the ${}^4F_{3/2} \rightarrow {}^4I_{9/2}$ manifold).

5. HIGHLY Nd-DOPED $GdVO_4$ LASER OUTPUT AT 1.06 AND 1.34 μm AT LOW PUMP POWER

A schematic of a DL-pumped Nd:$GdVO_4$ fundamental and intracavity frequency-doubled laser under low pump power is shown in Fig. 5. The pump source was an Optopower fiber-coupled diode laser with a center wavelength of 808 nm at a temperature of 25 °C. The maximum output power was 3 W, and the optical fiber diameter was 100 μm. A FiberPort adapter collimated the output from the end of the fiber, and a Special Optics laser diode collimator, with an aperture of 18 nm and a N.A. of 0.6, was used to focus the collimated beam into the laser crystal. The loss of the pump optics was ~8.3%, and the radius of the focused pump beam waist in the crystal was ~50 μm.

Nd:$GdVO_4$ crystal samples were polished to yield parallel flat surfaces, all 1 mm long and with 3 mm × 3 mm cross-sections. The flat front face of each laser crystal sample, which served as one of the resonator mirrors, was coated for high reflectivity (HR) at the lasing wavelength (1.06 or 1.34 μm) and for high transmission at the 808-nm pump wavelength. The flat exit face of each laser crystal was antireflection (AR) coated at the lasing wavelength to reduce intracavity reflection loss. The laser crystals were held upon copper mounts, with good thermal contact between crystal and mount to minimize the effects of pump heating. For 1.06-μm-laser operation, the laser resonator comprised a 20-mm radius-of-curvature output mirror and the 1.06-μm HR-coated surface of the laser crystal. The transmission of the output mirror was 5.0% at 1.06 μm. For 1.34-μm laser operation, the laser resonator consisted of a 20-mm radius-of-curvature output mirror and the 1.34-μm HR-coated surface of the laser crystal. Three output mirrors were coated, for 2.5%, 5.0%, and 10.0% transmission at 1.34 μm, and all had sufficient transmission (>90%) at 1.06 μm to suppress oscillation of the ${}^4F_{3/2} \rightarrow {}^4I_{11/2}$ transition.

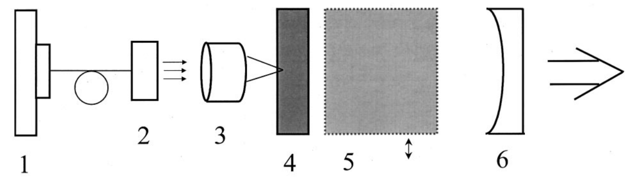

Fig. 5. Schematic of a LD-pumped highly Nd-doped Nd:$GdVO_4$ fundamental and intracavity frequency-doubled laser at low pump power: 1, LD, 2, FiberPort adapter; 3, Special Optics collomater; 4, laser crystal; 5, nonlinear crystal; 6, output mirror.

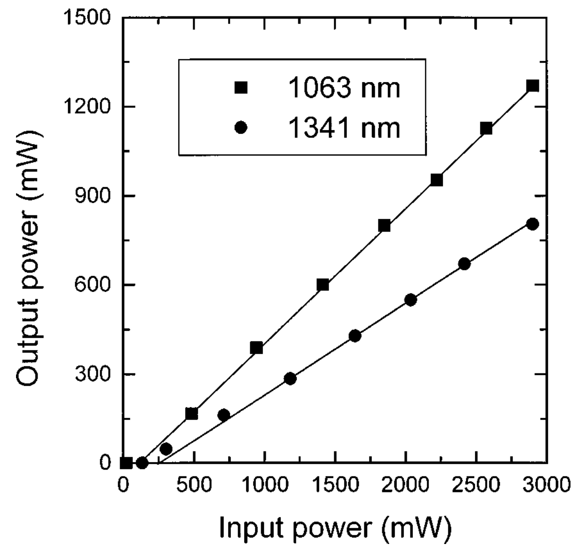

Fig. 6. Output powers of a highly Nd-doped Nd:$GdVO_4$ crystal at 1.06 and 1.34 μm as a function of input power at low pump power.

For 1.06- and 1.34-μm fundamental wavelength laser operation, the laser output power as a function of launched pump power is as shown in Fig. 6. With the same pump power of 2.9 W, 1.06-μm and 1.27-W output power and 1.34-μm 800-mW output power were obtained. The threshold pump power and the slope efficiency are measured to be 20 mW and 44.6% at 1.06 μm and 159 mW and 29.2% at 1.34 μm, respectively. The output beams for both 1.06 and 1.34 μm were linearly polarized and parallel to the *c* axis of the Nd:$GdVO_4$ crystal. Our experimental result for laser output power at 1.06 μm is higher than that reported by Jensen *et al.*[8] (the output power was 825 mW at the absorbed power of 1540 mW), and that for 1.34 μm is higher than that reported by Ostromov *et al.*[25] (the output power was 490 mW at an absorbed power of ~2200 mW).

6. SECOND HARMONIC GENERATION OF HIGHLY Nd-DOPED $GdVO_4$ CRYSTAL AT LOW PUMP POWER

For second-harmonic generation (SHG) of the 1.06-μm laser, a 5-mm-long KTP crystal with a cross section of

4 mm × 4 mm and oriented for type II phase matching ($\theta = 90°$ and $\varphi = 23.3°$) was inserted into the laser cavity. Both sides of the KTP crystal were polished to parallel flat surfaces and AR coating at 1.06 μm and 532 nm. The coating of the output mirror was changed to HR for 1.06 μm and AR for 532 nm, but the mirror's radius of curvature remained at 20 mm.

For SHG of the 1.34-μm laser, an 8-mm-long LBO crystal with a cross section of 3 mm × 3 mm and oriented for type I phase matching ($\theta = 84.8°$ and $\varphi = 0°$) was inserted into the laser cavity. Both sides of the LBO crystal were polished to parallel flat surfaces and AR coating at 1.34 μm. The coating of the output mirror was changed to HR for 1.34 μm and to AR for 670 nm and 1.06 μm, but the mirror's radius of curvature remained at 20 mm.

For SHG of the 1.06-μm and 1.34-μm lasers, 532- and 670-nm output powers versus the launched pump power are shown in Fig. 7. With the same pump power of 2.9 W, 532-nm 610-mW green light output power and 670-nm 82-mW red light output power were obtained. The threshold pump power and the total optical conversion efficiency were measured to be 5 mW and 21.0% at 532 nm and 12 mW and 2.8% at 670 nm, respectively. Our green laser output power was much higher than that reported by Jensen *et al.*[8] (The output power at 0.53 μm was 40 mW at an absorbed power of 1500 mW with KTP crystal used as a doubler). To our knowledge, the 82-mW red laser is the first red laser output obtained from a Nd:GdVO$_4$ crystal. The green and red light outputs have good long-term stability and round beam spots. Notice also that all the efficiencies in the 1.06-μm, 1.34-μm, SHG 532-nm, and SHG 670-nm laser experiments were calculated for diode-launched pump power; if the real crystal absorbed power were used, the efficiencies would be much higher.

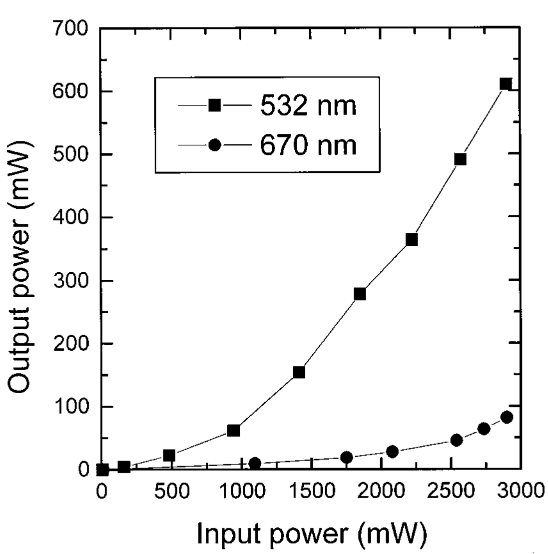

Fig. 7. Output powers of an intracavity frequency-doubled highly Nd-doped Nd:GdVO$_4$ crystal at 532 and 670 nm as a function of the input power at low pump power.

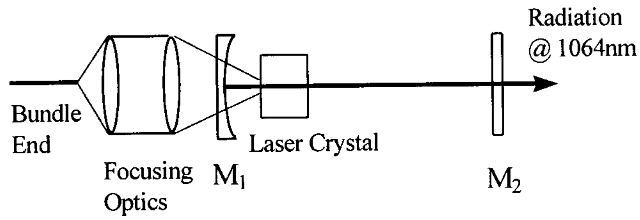

Fig. 8. Schematic of a LD-pumped highly Nd-doped Nd:GdVO$_4$ crystal for fundamental laser output at high pump power. M$_1$, M$_2$, mirrors.

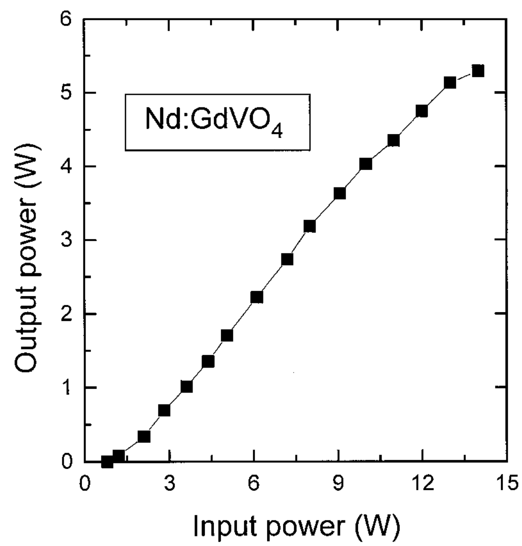

Fig. 9. Output power of highly Nd-doped Nd:GdVO$_4$ crystal at 1.06 μm as a function of the input power at high pump power.

7. HIGHLY Nd-DOPED GdVO$_4$ CRYSTAL LASER OUTPUT AT 1.06 μm AT HIGH PUMPING POWER

A laser experiment at 1.06 μm was performed with a 3-mm-thick crystal sample [the Nd doping concentration in the crystal was ~1.56 at. %; the dimensions of the crystal were 3 mm × 3 mm × 3 mm ($b \times c \times a$)]. The front face of the crystal was coated with a HR film at 1.06 μm and a high-transmission (HT) film at 0.8 μm, and the laser face was coated with a HT film at 1.06 μm. The pump source was a fiber-coupled cw LD array (OPC-D030-FCHS, Opto-power Corporation) that delivered a maximum output power of ~30 W at the fiber bundle end. The output beam from the fiber bundle end, which was 1.55 mm in diameter, was focused into the laser crystal with a spot size of ~0.775 mm and a N.A. of 0.22. A Nd:GdVO$_4$ crystal sample was wrapped with indium foil and held in a copper block, which was cooled by thermoelectric coolers. The efficiency of the focusing optics was 83%.

Figure 8 shows a schematic of the laser experiment. A plano–concave cavity is used in this optical system. Input coupler M_1 had a 20 cm radius of curvature and was coated with a HT film for 808 nm at the plate face, and the curvature face was coated with a HT film for 808 nm and a HR film for 1.06 μm. The output coupler (M_2) was a plate, and its transmission at 1.06 μm was 15%.

Figure 9 shows the measured output power of

Nd:$GdVO_4$ crystal samples versus the pump power. The highest output power of 5.29 W at 1.06 μm was achieved for a pump power of 14 W. The pump threshold was 0.32 W, the light–light conversion efficiency was 37.8%, and a slope efficiency of 45% was calculated from the curve. Our experimental results for output power and slope efficiency were higher than those reported by Wyss *et al.*[26] (Their output power was 5 W and their slope efficiency was 22%). Our pump threshold was lower than that reported by Wyss *et al.* (their pump threshold was 2.6 W).

8. LOW-Nd-DOPING CONCENTRATION $GdVO_4$ LASER OUTPUT AT 1.06 μm AND GREEN SHG AT 530 nm AT HIGH PUMP POWER AND ESTIMATION OF THE THERMAL-STRESS RESISTANCE FOM

The setup for low-Nd-doping concentration $GdVO_4$ laser output at 1.06 μm at high pump power is the same as in Fig. 8. An as-grown Nd:$GdVO_4$ crystal (0.5-at. % Nd in crystal) was cut into 3 mm × 3 mm × 4 mm crystal samples. (The 3 mm × 3 mm faces were polished; the light traveled along the 4-mm direction). The front face of the crystal sample was coated with a HT film at 0.8 and 1.06 μm, and the back faces were coated with HT film at 1.06 μm. The Nd:$GdVO_4$ crystal sample was wrapped with indium foil and held in a copper block, which was cooled by thermoelectric coolers.

Figure 10 shows the output power (the Nd-doping concentration in the $GdVO_4$ crystal was 0.5 at. %) versus the pump power for $T = 15\%$. From Fig. 10 we can see that the highest output power, as much as 14.25 W, of a Nd:$GdVO_4$ crystal is obtained at the highest pump power of 26 W. The light–light conversion efficiency was 54.8%, and the pump threshold was 0.32 W. A slope efficiency up to 62% was thus calculated from the linear part of the curve of the Nd:$GdVO_4$ crystal. The output beam quality at 14.3 W was measured to be $M^2 = 1.76$. The results that we obtained show that Nd:$GdVO_4$ is one of the best laser crystals for use in high-power laser systems.

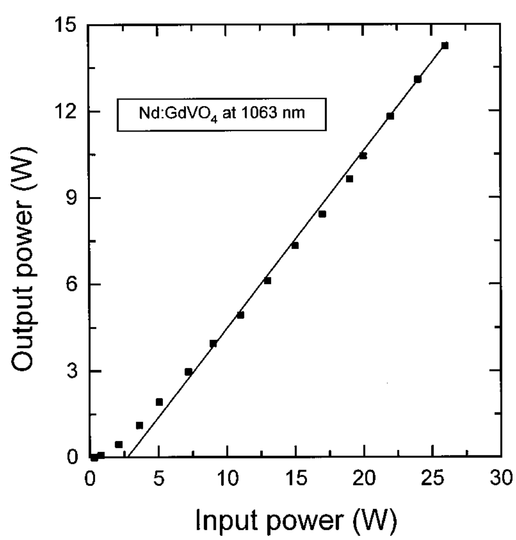

Fig. 10. Output power of a low-Nd-doping concentration Nd:$GdVO_4$ crystal at 1063 nm as a function of the input power at high pump power.

From the laser experiments with Nd:$GdVO_4$ at 1.06 μm described above, we can also estimate a thermal stress resistance FOM for a Nd:$GdVO_4$ crystal. From Refs. 16 and 27, we can obtain the following equation:

$$R_s = M_s \sigma_{\max} = \frac{(1 - v)k}{\alpha E} \frac{\alpha E \xi P_{\mathrm{abs}} \alpha_{\mathrm{abs}}}{4\pi(1 - v)k} = \frac{\xi P_{\mathrm{abs}} \alpha_{\mathrm{abs}}}{4\pi}, \tag{3}$$

where ξ is the fractional thermal loading, which depends on the choice of laser materials and on the corresponding pump source[28]; for Nd:$GdVO_4$, $\xi = 0.24$ $(1 - 808/1064 \approx 0.24)$. α_{abs} is the absorption coefficient of the laser crystal; in general, the absorption coefficient for a Nd-doped vanadate crystal can be written as $\alpha_{\mathrm{abs}} = 20 \times \mathrm{Nd}$,[27] where Nd is the concentration of Nd doping in the crystal. The absorption coefficient of a Nd:$GdVO_4$ crystal is larger than that of a Nd:YVO_4 crystal with the same Nd doping concentration; the absorption coefficient of 0.5-at.% Nd in a Nd:$GdVO_4$ crystal should be greater than 10($\alpha_{\mathrm{abs}} \geqslant 10$). From Fig. 10 we can see that the output power is not saturated at a pump power of 26 W, so we can estimate that the maximum pump power limitation of thermal fracture should be larger than the absorbed power of 30 W for a Nd:$GdVO_4$ crystal. We can also obtain that the value of R_s is larger than 5.73 W/cm for the Nd:$GdVO_4$ crystal, and, from Eq. (1), P_a/l of the Nd:$GdVO_4$ crystal is greater than 51.57 W/cm. The estimated FOM value of thermal-stress resistance in Nd:$GdVO_4$ crystal is similar to that of a Nd:Cr:$Gd_3Sc_2Ga_3O_{12}$ crystal (6.6 W/cm), and it is approximately half that of an ($Y_3Al_5O_{12}$, 11 W/cm) crystal.[29] These results show that a Nd:$GdVO_4$ crystal is robust to rupture from thermal stresses and can be used in high-power laser systems.

From Figs. 9 and 10 we can see that, 1.56 at. %, Nd:$GdVO_4$ has less output power and efficiency than at 0.5 at. %. This result indicates that at 1.56 at. % a Nd:$GdVO_4$ crystal is not suitable for use in a high-power cw LD laser system. That this is so can be explained as follows: The absorbed pump power at the thermal fracture limit ($P_{\mathrm{abs,lim}}$) is[27]

$$P_{\mathrm{abs,lim}} = \frac{1}{\alpha_{\mathrm{abs}}} \frac{4\pi R_s}{\xi}. \tag{4}$$

From Eq. (4) one can know that $P_{\mathrm{abs,lim}} \propto 1/\alpha_{\mathrm{abs}}$, which means that the absorption coefficient is an important factor that influences the scope of absorbed power of a laser crystal; the higher the Nd-doping concentration in Nd:$GdVO_4$, the less the absorbed pump power at the thermal fracture limit of a Nd:$GdVO_4$ crystal, so 0.5-at. % Nd:$GdVO_4$ is suitable for use in a high-pump-power laser system. We used a 0.5-at. % Nd:$GdVO_4$ crystal to demonstrate green laser output at 532 nm, actively Q-switched laser output at 1.06 μm, and actively Q-switched green laser output at 532 nm at high pump power.

The experimental setup for green laser output at 0.53 μm is shown in Fig. 11. Input coupler M_1 had a 15-cm radius of curvature and was coated with HT film for 808

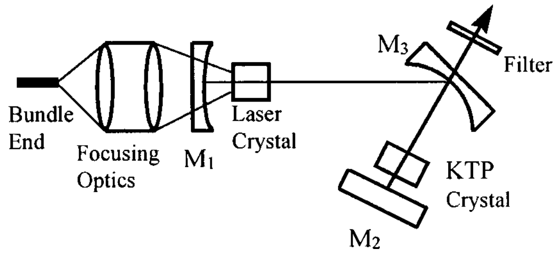

Fig. 11. Schematic of a LD-pumped low-Nd-doping concentration $Nd:GdVO_4$ intracavity frequency-doubled laser at high pump power. M_1–M_3, mirrors.

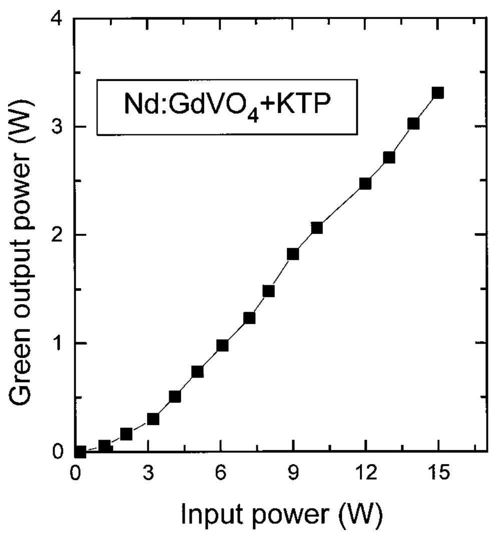

Fig. 12. Output powers of an intracavity frequency-doubled low-Nd-doping concentration $Nd:GdVO_4$ crystal at 532 nm as a function of input power at high pump power.

nm at the plate face, and the curvature face was coated with a HT film for 808 nm and a HR film for 1.06 μm. Coupler M_3 had a 10-cm radius of curvature and was coated with AR film for 0.53 μm at the plate face, and the curvature face was coated with a HT film for 0.53 μm and a HR film for 1.06 μm. M_2 was a flat mirror, and it was coated with HR film at 1.06 μm and at 0.53 μm. The $Nd:GdVO_4$ crystal sample was the same as that in the laser experiment with low-Nd-doping concentration $Nd:GdVO_4$ crystal at high pump power at 1.06 μm. A 3 mm × 3 mm × 11 mm KTP crystal was cut for type II phase matching at 1.06 μm. It was AR coated for 1.06 μm on one end face and 0.53 μm on the other and was used as an intracavity frequency doubler. The $Nd:GdVO_4$ and KTP crystal samples were wrapped with indium foil and held in a copper block, which was cooled by thermoelectric coolers. The pump source was the same as that in the fundamental experiment. Figure 12 shows an output power of 0.53 μm. From the figure we can see that the threshold of green laser output is 0.2 W; 3.3-W green laser output power was obtained at a pump power of 15 W. The highest light–light conversion efficiency was 22%. The quality factor of the output beam at a green power of 3.3 W was $M^2 = 1.55$. To our knowledge, this is the highest green output power at 0.53 μm for a $Nd:GdVO_4$ crystal when a KTP crystal is used as a doubler.

9. *Q*-SWITCHED LASER OUTPUT AT 1.06 AND 0.53 μm FOR $Nd:GdVO_4$ CRYSTAL

The increasing demand for cheap and compact pulsed solid-state lasers has led to a number of recent developments in actively and passively *Q*-switched lasers.[26,30,31] Passively *Q*-switched laser output of a $Nd:GdVO_4$ crystal at 1.06 μm has been demonstrated.[32] Now we demonstrate the acousto-optical *Q*-switched laser output of a $Nd:GdVO_4$ crystal at 1.06 and 0.53 μm.

A schematic of the *Q*-switched experiment at 1.06 μm is shown in Fig. 13. An acousto-optical *Q* switch that was 24 mm long and had an AR coating at 1.06 μm on both faces was inserted into the cavity. It was placed behind and close to the $Nd:GdVO_4$ crystal. The $Nd:GdVO_4$ crystal had a 0.5-at. % Nd doping concentration in the crystal, whose dimensions were 3 mm × 3 mm × 4 mm. The crystal was wrapped with indium foil and held in a copper block, which was cooled by thermal coolers.

Figure 14 shows the average output power of 1.06 μm at a *Q*-switching repetition frequency of 60 kHz as a function of incident pump power for 30% output coupling. The highest output power was 7.25 W at a pump power of 19 W, the pumping threshold was 1.3 W, the optical–optical conversion efficiency was 38.1%, and the slope efficiency of 42.9% was calculated from Fig. 14.

The crystal sample and a schematic of the setup for the SHG *Q*-switching experiment at 0.53 μm are shown in

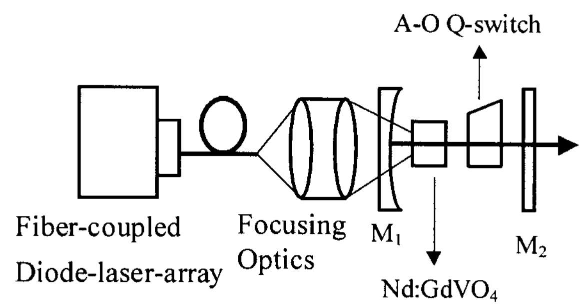

Fig. 13. Schematic an end-pumped *Q*-switched 1.06-μm $Nd:GdVO_4$ laser. M_1, M_2, mirrors; A-O, acousto-optical.

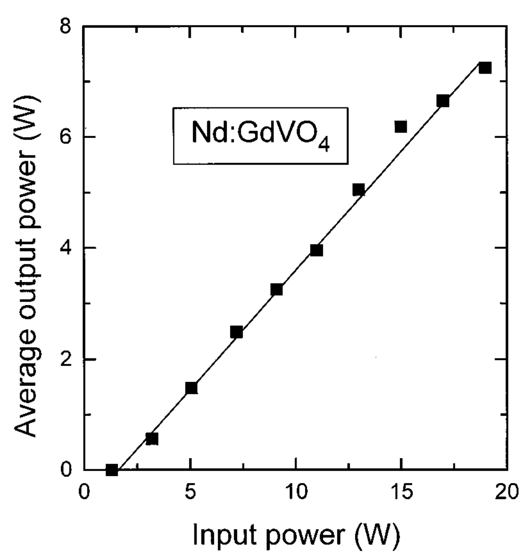

Fig. 14. Average output power at 1.06 μm and a pulse repetition frequency of 60 kHz as a function of incident pump power.

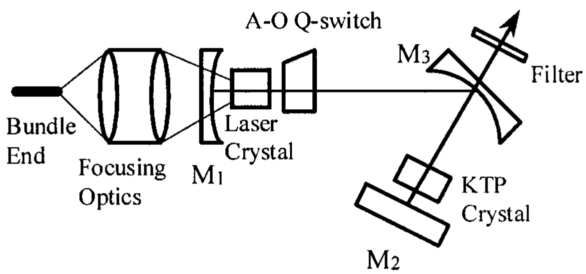

Fig. 15. Schematic of an end-pumped Q-switched intracavity frequency-doubled $Nd:GdVO_4$/KTP green laser. M_1–M_3, mirrors; A-O, acousto-optical.

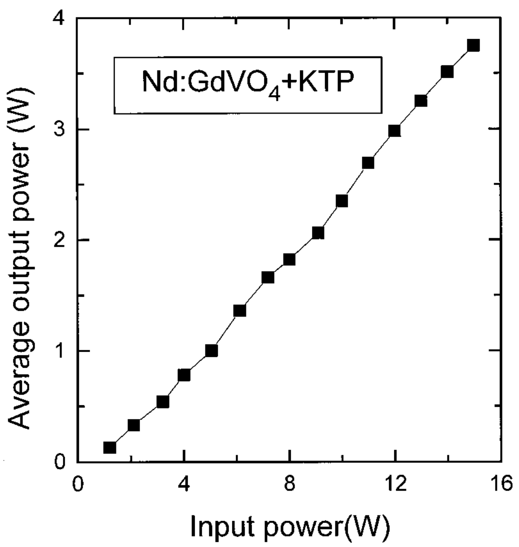

Fig. 16. Average output power at 532 nm at a pulse repetition frequency of 50 kHz as a function of incident pump power.

Fig. 15. A KTP crystal with the dimensions 3 mm × 3 mm × 15 mm was cut for type II phase matching; its coating films were the same as for the KTP crystal and had dimensions of 3 mm × 3 mm × 11 mm. An acousto-optical Q switch was inserted into the cavity, placed behind and close to the $Nd:GdVO_4$ crystal. The crystal had a 0.5-at. % Nd doping concentration, and its dimensions were 3 mm × 3 mm × 4 mm. Both $Nd:GdVO_4$ and KTP crystals were wrapped with indium foil and held in a copper block, which was cooled by thermal coolers.

Figure 16 shows an average output power of 0.53 μm at a Q-switching repetition frequency of 50 kHz as a function of incident pump power. The highest output power at 532 nm was 3.75 W at a pump power of 15 W, and the optical–optical conversion efficiency was 25%. The optical–optical conversion efficiency of pulsed green laser output is higher than that of cw green laser output.

10. THERMAL LENSING MEASUREMENT OF $Nd:GdVO_4$ CRYSTAL

In high-power solid-state lasers, pump-induced thermal focusing is of primary importance because of its significant influence on almost all major aspects of these lasers. For a given laser resonator configuration, the performance of the solid-state laser is actually dominated by thermal lensing in the laser medium. Therefore, determining the thermal focal lengths at various pump power levels is essential for the design and optimization of solid-state lasers. In this section we describe a simple method for measuring the pump-induced thermal focal length of a laser crystal.[33] This method is based on a conclusion deduced from the stability theory of resonators. A schematic of the setup for measuring the thermal focal length is shown in Fig. 17. M_1 is a plane mirror with one surface AR coated at 808 nm and the other surface HR coated at 1064 nm and HT coated at 808 m. M_2 is a plane mirror with 2% transmission at 1064 nm and serves as the output coupler. For ease in moving M_2 back and forth, we mounted M_2 upon a translation stage. The laser crystals employed in this experiment were $Nd:GdVO_4$ (3 mm × 3 mm × 4 mm) and $Nd:YVO_4$ (3 mm × 3 mm × 5 mm; also grown by the Czochralski method in our laboratory), with 0.5-at. % Nd doping crystals. Both crystals were AR coated at 808 nm and 1.06 μm on the pump faces and at 1.06 μm on the opposite faces. To extract the heat generated in the crystal at high-pump-power levels we wrapped the crystals with indium foil and held them in a copper block that was cooled by thermoelectric coolers. The pump LD was the same as that in Fig. 8. But the output beam from the bundle end was focused into the laser crystal with a spot radius of ~0.4 mm. We measured the thermal focal lengths (f_T) of the end-pumped $Nd:GdVO_4$ crystal in the range of incident pump power from 10 to 22 W. For comparison, thermal lensing of $Nd:YVO_4$ crystal at incident pump powers that ranged from 6 to 18 W was also measured.

Figure 18 shows the thermal focal power ($1/f_T$) as a

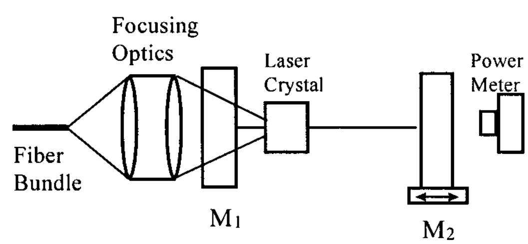

Fig. 17. Schematic of the setup for measuring thermal focal length. M_1, M_2, mirrors.

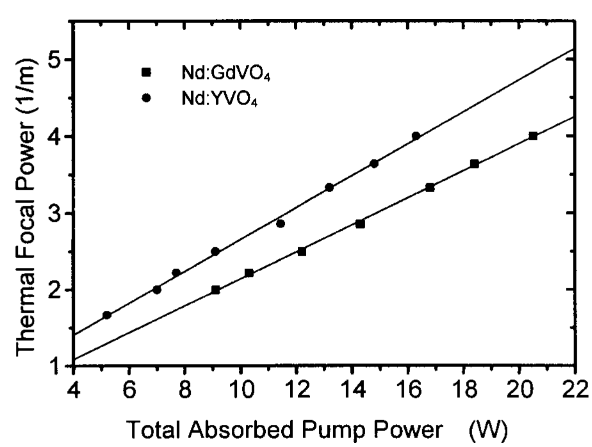

Fig. 18. Thermal focal power versus total absorbed pump power for $Nd:GdVO_4$ and $Nd:YVO_4$ crystals with the same concentration of Nd dopant.

function of total absorbed pump power. It can be seen that the thermal lensing of Nd:$GdVO_4$ is considerably weaker than that of Nd:YVO_4, in agreement with the fact that the thermal conductivity of Nd:$GdVO_4$ is much higher than that of Nd:YVO_4.

We could also estimate the temperature-induced changes in the refractive index ($\mathrm{d}n/\mathrm{d}T$) of Nd:$GdVO_4$ crystal by using the thermal focal length. From Ref. 34, the thermal focal length of a laser crystal can be written as

$$f = \frac{\pi k \omega_p^2}{P_{\mathrm{th}}(\mathrm{d}n/\mathrm{d}T)}\left(\frac{1}{1 - \exp(-\alpha_{\mathrm{abs}} l)}\right), \tag{5}$$

where k is the thermal conductivity, ω_p is the radius of the pump-beam, P_{ph} is the fraction of pump power that results in heating, $P_{\mathrm{th}} = \xi P_{\mathrm{abs}} = 0.24 \quad P_{\mathrm{abs}}$ $(1 - 808/1064 \approx 0.24)$, P_{abs} is the absorption power of the laser crystal, α_{abs} is the absorption coefficient of the laser crystal, and l is the length of the laser crystal. In general, $\alpha_{\mathrm{abs}} l > 4$, so $l - \exp(-\alpha_{\mathrm{abs}} l) \approx 1$.

We can obtain the expression far $\mathrm{d}n/\mathrm{d}T$:

$$\frac{\mathrm{d}n}{\mathrm{d}T} = \frac{\pi k \omega_p^2}{P_{\mathrm{th}} f}. \tag{6}$$

From Fig. 18, when the absorbed pump power is 22 W for Nd:$GdVO_4$ we can obtain an estimated value for $\mathrm{d}n/\mathrm{d}T$ of $4.7 \times 10^{-6}\,\mathrm{K}^{-1}$; when the absorbed pump power is 16 W for Nd:YVO_4 the value of $\mathrm{d}n/\mathrm{d}T$ is $2.7\times10^{-6}\,\mathrm{K}^{-1}$, in agreement with that reported in the literature[12] (the value of $\mathrm{d}n/\mathrm{d}T$ is $3\times10^{-6}\,\mathrm{K}^{-1}$ for Nd:YVO_4 crystal).

11. CONCLUSIONS

Our study has shown that a Nd:$GdVO_4$ single crystal can be grown by the Czochralski method. The thermal expansion coefficients of Nd:$GdVO_4$ from 298 to 572.5 K are $\alpha_1 = 1.5 \times 10^{-6}$/K and $\alpha_3 = 7.3 \times 10^{-6}$/K. The specific heat of Nd:$GdVO_4$ is 32.6 cal(mol K) at 330 K. The estimated material constant of Nd:$GdVO_4$ is $8.07 \times 10^{-6}\,\mathrm{m}^2/\mathrm{s}$, and that of Nd:$YVO_4$ is $3.14 \times 10^{-6}\,\mathrm{m}^2/\mathrm{s}$. The spectral experiments show that a Nd:$GdVO_4$ crystal can be pumped by an 808.5-nm LD and produce laser output at 1.06 and 1.34 μm at room temperature. The laser outputs of highly Nd-doped Nd:$GdVO_4$ at 1.06 and 1.34 μm were obtained with low-power LD pumping. The output power at 1.06 μm was 1.27 W for a pump power of 2.9 W, the pumping threshold was 64 nm, and the slope efficiency was 44.6%. The output power at 1.34 μm was 800 mW for a pump power of 2.9 W, the pumping threshold was 159 mW, and the slope efficiency was 29.2%. The SHG green laser output power at 532 nm was 610 mW for a pump power of 2.9 W, the pumping threshold was 5 mW, and the optical–optical conversion efficiency was 21.0%. The SHG red laser output power at 670 nm was 82 mW for a pump power of 2.9 W, the pumping threshold was 12 mW, and the optical–optical conversion efficiency was 2.8%. At a pump power of 14 W, the output power of a 1.56 at. % Nd-doping concentration in Nd:$GdVO_4$ was 5.29 W, the pumping threshold was 0.32 W, and the slope efficiency was 45%. The laser output power of a low-Nd-doping concentration Nd:$GdVO_4$ at 1.06 μm was 14.25 W at the highest pump power of 26 W, the light–light conversion efficiency was 54.8%, the pumping threshold was 0.32 W, and the slope efficiency was 62%. The laser output power of a low-Nd-doping concentration Nd:$GdVO_4$ crystal at 532 nm was 3.3 W for a pump power of 15 W, the threshold of the green laser output was 0.2 W, and the highest optical–optical conversion efficiency was 22%. The low-Nd-doping concentration Nd:$GdVO_4$ crystal is therefore more suitable than the highly doped crystal for use in a high-pump-power laser system. The average Q-switched laser output power at 1.06 μm was 7.25 W at a pump power of 19 W, the pumping threshold was 1.3 W, the optical–optical conversion efficiency was 38.1%, and the average slope efficiency was 42.9%. The average Q-switched green laser output power was 3.75 W at a pump power of 15 W, and the optical–optical conversion efficiency was 25%. The thermal lens of a Nd:$GdVO_4$ crystal was measured, and it was weaker than that of a Nd:YVO_4 crystal. Some important parameters of Nd:$GdVO_4$ crystal have been calculated or estimated: $\mathrm{d}n/\mathrm{d}T = 4.7 \times 10^{-6}\,\mathrm{K}^{-1}$; material constant, $3.5 \times 10^{-6}\,\mathrm{m}^2/\mathrm{s}$; FOM of the thermal-stress resistance, >5.73 W/cm, power per unit length at the stress limit, 51.57 W/cm. The results described above have shown that Nd:$GdVO_4$ crystal is a good laser crystal for producing 1.06- and 1.34-μm laser output in high-power cw and pulsed laser systems.

ACKNOWLEDGMENTS

The authors thank Z. H. Yang for his measurements of thermal properties and optical spectra. This research is partly supported by the National Natural Science Foundation of China (grant 59823003), the Research Award Foundation for Prominent Youth Scientists of Shandong Province, the Key Program of Science and Technology Research of the Ministry of Education of China, and a Hong Kong University grants.

H. Zhang's email address is huaijin@hotmail.com.

REFERENCES

1. J. R. O'Connor, "Unusual crystal-field energy levels and efficient laser properties of YVO_4:Nd," Appl. Phys. Lett. **9**, 407–409 (1966).
2. A. W. Tucher, M. Birnbaum, C. L. Fincher, and L. G. Deshazer, "Continuous-wave operation of Nd:YVO_4 at 1.06 and 1.34 μm," J. Appl. Phys. **47**, 232–234 (1976).
3. A. W. Tucher, M. Birebaun, C. L. Fincher, and J. W. Erler, "Stimulated-emission cross section at 1064 and 1342 nm in Nd:YVO_4," J. Appl. Phys. **48**, 4907–4911 (1977).
4. R. A. Fielfs, M. Birnbaun, and C. L. Fincher, "Highly efficient Nd:YVO_4 diode-laser end-pumped laser," Appl. Phys. Lett. **51**, 1885–1886 (1987).
5. T. Izawa, R. Uchimura, S. Matsui, T. Arichi, and T. Yakouh, "Efficient diode bar-pumped intracavity-doubled Nd:YVO_4 laser using stacked-glass plate beam shaper," in *Conference on Lasers and Electro-Optics (CLEO/U.S.)*, Vol. 6 of 1998 OSA Technical Digest Series (Optical Society of America, Washington, D.C., 1998), paper CThA1.
6. U. Nebel, B. Ruffing and R. Wallenstein, "A high power diode-pumped all-solid-state RGB laser source," in *Conference on Lasers and Electro-Optics (CLEO/U.S.)*, Vol. 6 of

1998 OSA Technical Digest Series (Optical Society of America, Washington, D.C., 1998), pp. CPD3-1–CPD3-3.

7. A. I. Zagmennyi, V. G. Ostromov, I. A. Shcherbarkov, T. Jensen, J.-P. Meyn, and G. Huber, "The Nd:$GdVO_4$ crystal: a new material for diode pumped lasers," Sov. J. Quantum Electron. **22**, 1071–1072 (1992).
8. T. Jensen, V. G. Ostroumov, J.-P. Meyn, G. Huber, A. I. Zagumennyi, and I. A. Scherbakov, "Spectroscopic characterization and laser performance of diode-laser-pumped Nd:$GdVO_4$," Appl. Phys. B **58**, 373–379 (1994).
9. K. Shimamura, S. Uda, V. V. Kochurikhin, T. Taniuchi, and T. Fukuda, "Growth and characterization of gadolinium vanadate $GdVO_4$ single crystal for laser applications," Jpn. J. Appl. Phys. **35**, 1832–1835 (1996).
10. H. J. Zhang, X. L. Meng, L. Zhu, H. Z. Zhang, P. Wang, J. Dawes, C. Q. Wang, Y. T. Chow, "Investigation on the growth and laser properties of Nd:$GdVO_4$ single crystal," Cryst. Res. Technol. **33**, 801–806 (1998).
11. P. A. Studenikin, A. I. Zagumennyi, Yu. D. Zavartsev, P. A. Popov, and I. A. Shcherbakov, "$GdVO_4$ as a new medium for solid-state lasers: some optical and thermal properties of crystals doped with Nd^{3+}, Tm^{3+}, and Er^{3+} ions," Quantum Electron. **25**, 1162–1165 (1995).
12. B. H. T. Chai, G. Loutts, J. Lefaucheur, X. X. Zhang, P. Hong, M. Bass, I. A. Shcherbakov, and A. I. Zagumennyi, "Comparison of laser performance of Nd-doped YVO_4, $GdVO_4$, $Ca_5(PO_4)_3F$, $Sr_5(PO_4)_3F$ and $Ca_5(VO_4)_3F$," in *Advanced Solid-State Lasers*, T. Y. Fan and B. H. T. Chai, eds., Vol. 20 of OSA Trends in Optics and Photonics Series (Optical Society of America, Washington, D.C., 1994), pp. 41–52.
13. X. Meng, L. Zhu, H. Zhang, C. Wang, Y. T. Chow, and M. Lu, "Growth, morphology and laser properties of Nd:YVO_4 crystal," J. Cryst. Growth **200**, 199–203 (1999).
14. Joint Committee for Power Diffraction Standards diffraction file: 17–260.
15. H. Zhang, X. Meng, L. Zhu, C. Wang, Y. T. Chow, and M. Lu, "Growth, spectra and influence of annealing effect on laser properties of Nd:YVO_4 crystal," Opt. Mater. **14**, 25–30 (2000).
16. J. M. Eggleston, T. J. Kane, K. Kuhn, J. Unternahere, and R. L. Byer, "The slab geometry laser. I. Theory." IEEE J. Quantum Electron. **QE-20**, 289–301 (1984).
17. D. Xiao and M. Wang, *Crystal Physics* (Sichuan U. Press, Chengdu, China, 1989; in Chinese), p. 3.
18. X. Peng, A. Asundi, Y. Chen, and Z. Xiong, "Study of the mechanical properties of Nd:YVO_4 crystal by use of laser interferometry and finite-element analysis," Appl. Opt. **40**, 1396–1403 (2001).
19. D. Xu, "Organic crystal," in *Science and Technology of Crystal Growth*, K. C. Zhang and L. H. Zhang, eds. (Science Press, Beijing, 1997; in Chinese), p. 328.
20. H. J. Zhang, L. Zhu, X. L. Meng, Z. H. Yang, C. Q. Wang, W. T. Yu, Y. T. Chow, and M. K. Lu, "Thermal and laser properties of Nd:YVO_4 crystal," Cryst. Res. Technol. **34**, 1011–1016 (1999).
21. T. Y. Fan and R. L. Byer, "Modeling and cw operation of a quasi-three-level 946 nm Nd:YAG laser," IEEE J. Quantum Electron. **23**, 605–612 (1987).
22. W. P. Risk, "Modeling of longitudinally pumped solid-state lasers exhibiting reabsorption losses," J. Opt. Soc. Am. B **5**, 1412–1423 (1988).
23. J. H. Zarrabi, P. Gavrilovic, and S. Singh, "Intracavity, frequency-doubled, miniaturized Nd:$YAlO_3$ blue laser at 465 nm," Appl. Phys. Lett. **67**, 2439–2441 (1995).
24. P. Zeller and P. Peuser, "Efficient, multiwatt, continuous-wave laser operation on the $^4F_{3/2}$–$^4I_{9/2}$ transitions of Nd:YVO_4 and Nd:YAG," Opt. Lett. **25**, 34–36 (2000).
25. V. G. Ostroumov, J.-P. Meyn, T. Jensen, and G. Huber, "Neodymium-doped 1.3-μm and GVO laser and 1.4-μm YAG lasers," in *Conference on Laser and Electro-Optics*, Vol. 15 of OSA 1995 Technical Digest Series (Optical Society of America, Washington, D.C., 1995), paper CWH6.
26. Chr. P. Wyss, W. Luthy, H. P. Weber, V. L. Vlasov, Yu. D. Zavrtsev, P. A. Studenokin, and A. I. Zagumennyi, "Performance of a diode-pumped 5 W Nd^{3+}:$GdVO_4$ microchip laser at 1.06 μm," Appl. Phys. B **68**, 659–661 (1999).
27. Y.-F. Chen, "Design criteria for concentration optimization in scaling diode end-pumped lasers to high power: influence of thermal fracture," IEEE J. Quantum Electron. **25**, 234–239 (1999).
28. R. Weber, B. Neuenschwander, M. Mac Donald, M. B. Roos, and H. P. Weber, "Cooling schemes for longitudinally diode laser-pumped Nd:YAG rpds," IEEE J. Quantum Electron. **34**, 1046–1053 (1998).
29. W. F. Krupke, M. D. Shinn, J. E. Marion, J. A. Caird, and S. E. Stokowski, "Spectroscopic, optical, and thermomechanical properties of neodymium- and chromium-doped gadolinium scandium gallium garnet," J. Opt. Soc. Am. B **3**, 102–113 (1986).
30. A. Agnesi, S. Dell'Acqua, C. Pennacchio, G. Reali, and P. G. Gobbi, "High-repetition-rate *Q*-switched diode-pumped Nd:YAG laser at 1.444 μm," Appl. Opt. **37**, 3984–3986 (1998).
31. I. D. Lindsay and M. Ebrahimzdeh, "Efficient coutinous-wave and *Q*-switched operation of a 946-nm Nd:YAG laser pumped by an injection-locked broad-area diode laser," Appl. Opt. **37**, 3961–3970 (1998).
32. G. J. Friel, R. S. Conroy, A. J. Kemp, B. D. Sinclair, and J. M. Ley, "*Q*-switching of a diode-pumped Nd:YVO_4 laser using a quadrupole electro-optic deflector," Appl. Phys. B **67**, 267–270 (1998).
33. J. Liu, J. Lu, J. Lu, Z. Shao, and M. Jiang, "Thermal lens determination of end-pumped solid-state lasers by a simple direct approach," Chin. Phys. Lett. **16**, 181–183 (1999).
34. M. E. Innocenzi, H. T. Yura, C. L. Fincher, and R. A. Fields, "Thermal modeling of continuous-wave end-pumped solid-state lasers," Appl. Phys. Lett. **56**, 1831–1833 (1990).